Electronic Supplementary Information

Mitochondria-targeted half-sandwich ruthenium^{II} diimine complexes: anticancer and antimetastasis via ROS-mediated signalling

Zhishan Xu[a,b], Deliang Kong[a], Xiangdong He[a], Lihua Guo[a], Xingxing Ge[a], Xicheng Liu[a], Hairong zhang[a], Juanjuan Li[a], Yuliang Yang[a], Zhe Liu[a*]

[a] Institute of Anticancer Agents Development and Theranostic Application, The Key Laboratory of Life-Organic Analysis and Key Laboratory of Pharmaceutical Intermediates and Analysis of Natural Medicine, Department of Chemistry and Chemical Engineering, Qufu Normal University, Qufu 273165, China.

[b] College of Chemistry, Chemistry Engineering and Materials Science, Shandong Normal University, Jinan 250014, China.

*Corresponding author. Email: liuzheqd@163.com

Abstract

Supporting information includes the experimental details and data. The experimental section includes the materials and instruments, the synthesis of the ligands ($\mathbf{L_1}$-$\mathbf{L_2}$) and complexes **[(η^6-p-cymene)Ru(L1)Cl]PF_6 (Ru1)** and **[(η^6-p-cymene)Ru(L2)Cl]PF_6 (Ru2)**. Experimental data include the BSA interactions, catalytic hydride transfer analysis, cell toxicity, cell cycle, cellular distribution, apoptosis, mitochondrial membrane, ROS induction, caspase 3/PARP activity and antimetastasis assay.

EXPERIMENTAL SCETION

Materials and Instrumentation. All the synthesis operations were performed in a nitrogen atmosphere. $RuCl_3 \bullet nH_2O$, α-terpinene, 2, 3-butanedione, p-Toluidine, or 4-bromoaniline, BSA and NADH were purchased from Sigma-Aldrich. For the biological experiments, DMEM medium, fetal bovine serum, penicillin/streptomycin mixture, trypsin/EDTA, cisplatin, MTT, and phosphate-buffered saline (PBS) were purchased from Sangon Biotech. Testing compounds was dissolved in DMSO and diluted with the tissue culture medium before use. Stock solutions of cisplatin (10 mM) and complexes **Ru 1–2** (10 mM) were prepared in PBS and DMSO, respectively. All stock solutions were stored at -20 °C, thawed and diluted with culture medium prior to each experiment.

NMR Spectroscopy. ^{1}H NMR spectra were acquired in 5 mm NMR tubes at 298 K on Bruker DPX 500 (^{1}H = 500.13 MHz) spectrometers. ^{1}H NMR chemical shifts were internally referenced to $(CHD_2)(CD_3)SO$ (2.50 ppm) for DMSO-d_6, $CHCl_3$ (7.26 ppm) for chloroform-d_1. All data processing was carried out using XWIN-NMR version 3.6 (Bruker UK Ltd.).

UV-Vis Spectroscopy. The UV-Vis spectra of the compounds were recorded by TU-1901 UV spectrophotometer with 1 cm path-length quartz cuvettes (3 ml). Spectra were processed using UVWinlab software. Experiments were carried out at 298 K unless otherwise stated.

Zeta Potential analysis. Zeta potentials of the **Ru1** and **Ru2** were measured using a Delsa Nano C (Beckman Coulter Ltd, USA). The concentration of complexes Ru was 0.1mg/ml in EtOH. Prior to each measurement, the operating conditions were checked and adjusted.

Reaction with NADH. The reaction of complexes **Ru1** and **Ru2** (ca. 1 μM) with NADH (ca. 83 μM) in 10% MeOH/90% H_2O (v/v) was monitored by UV-Vis at 298 K after various time intervals. TON was calculated from the difference in NADH concentration after 8 h divided by the concentration of ruthenium catalyst. The concentration of NADH was obtained using the extinction coefficient $\varepsilon_{339} = 6220\ M^{-1}cm^{-1}$.

Cell Culture. HeLa cells, A549 cells, A549cisR cells HT29 cells, HCT116 cells, HepG2 cells and CT26 cells were obtained from Shanghai Institute of Biochemistry and Cell Biology (SIBCB) and were grown in Dubelco's Modified Eagle Medium (DMEM). All media were supplemented with 10% fetal bovine serum, and 1% penicillin-streptomycin solution. All cells were grown at 310 K in a humidified incubator under a 5 % CO_2 atmosphere.

Colony Formation Assay. After plating 1000 of A549 cancer cells per well in 12-well plates, cells treated with the concentrations of $0.125 \times IC_{50}$ and $0.25 \times IC_{50}$ of complexes **Ru1** and **Ru2** were cultured for 10 days for the development of macroscopic colonies. The plates were washed three times with PBS and fixed with 4% paraformaldehyde for 20 min. All cells were stained with 0.1% crystal violet, washed with distilled water to remove excess stain. Experiments were set up in triplicate, and the medium was changed every 3 days.

Colocalization assay. A549 cells (5×10^5 /2 ml per well) were seeded in a six-well plate. Cells were preincubated in drug-free media at 310 K for 24 h, after which complexes **Ru1** and **Ru2** was added at concentration $1 \times IC_{50}$ to a six-well plate for different time intervals, and then cells were incubated with MTDR (100 nM) at 310 K for 30 min. Cells were washed three times with ice-cold PBS and visualized by confocal microscopy (LSM 880 NLO, Carl Zeiss, Germany) immediately. Ru complexes were excited at 488 nm and MTDR was excited at 633 nm, respectively. Emission was collected at 520 ± 20 nm (Ru complexes) and 710 ± 20 nm (MTDR), respectively.

Viability assay (MTT assay). After plating 5000 A549 cells per well in 96-well plates, the cells were preincubated in drug-free media at 310 K for 24 h before adding different concentrations of the compounds to be tested. In order to prepare the stock solution of the drug, the solid complexes **Ru1** and **Ru2** were dissolved in DMSO. This stock was further diluted using cell culture medium until working concentrations were achieved. The drug exposure period was 24 h. Subsequently, 15 μl of 5 mg ml^{-1} MTT solution was added to form a purple formazan. Afterwards, 100 μl of dimethyl sulfoxide (DMSO) was transferred into each well to dissolve the

purple formazan, and results were measured using a microplate reader (DNM-9606, Perlong Medical, Beijing, China) at an absorbance of 570 nm. Each well was triplicated and each experiment repeated at least three times. IC_{50} values quoted are mean ± SEM.

Cell Cycle Analysis. The A549 cancer cells at 1.0×10^6 per well were seeded in a six-well plate. Cells were preincubated in drug-free media at 310 K for 24 h, after which complexes **Ru1** and **Ru2** were added at concentrations of $0.25 \times IC_{50}$, $0.5 \times IC_{50}$, $1 \times IC_{50}$ and $2 \times IC_{50}$ of complexes Ru1 and Ru2 against A549 cancer cells. After 24 h of drug exposure, supernatants were removed by suction and cells were washed with PBS. Finally, cells were harvested using trypsin-EDTA and fixed for 24 h using cold 70% ethanol. DNA staining was achieved by resuspending the cell pellets in PBS containing propidium iodide (PI) and RNase. Cell pellets were washed and resuspended in PBS before being analyzed in a flow cytometer (ACEA NovoCyte, Hangzhou, China) using excitation of DNA-bound PI at 488 nm, with emission at 585 nm. Data were processed using NovoExpress™ software. The cell cycle distribution is shown as the percentage of cells containing G_0/G_1, S and G_2/M DNA as identified by PI staining.

Induction of Apoptosis. Flow cytometry analysis of apoptotic populations of the cells caused by exposure to iridium complexes was carried out using the Annexin V-PE/7-AAD Apoptosis Detection Kit (KeyGEN BioTECH, China) according to the supplier's instructions. Briefly, A549 cancer cells (1.0×10^6 /2 ml per well) were seeded in a six-well plate. Cells were preincubated in drug-free media at 310 K for 24 h, after which complexes **Ru1** and **Ru2** was added at concentrations of $0.5 \times IC_{50}$, $1 \times IC_{50}$ and $2 \times IC_{50}$ to a six-well plate. After 24 h of drug exposure, cells were collected and washed once with PBS, and resuspended in 195 µl of annexin V-PE binding buffer which was then added to 5 µl of 7-AAD and 1 µl of annexin V-PE, and then incubated at room temperature in the dark for 15 min. Subsequently, the buffer placed in an ice bath in the dark. The samples were analyzed by a flow cytometer (ACEA NovoCyte, Hangzhou, China).

Cellular distribution assay. A549 cells were seeded in 100 mm dishes for 24 h, then the media was removed and replaced with fresh media containing the tested complexes **Ru1** and **Ru2** at concentration 10 µM for 24 h. After the removal of the culture media and rinse with 1 mL of PBS buffer (1X), the cells were treated with 500 µl of 0.25% trypsin and centrifuged at 1000 rpm. The cells were counted using the automated cell counter and were used for cytoplasmic, membrane, nuclear soluble, chromatin-bound and cytoskeletal protein fractionation, subcellular protein fractionation kit for cultured cells (Thermo scientific, USA). Fractionations were digested with concentrated nitric acid (65%, 50 µl) at 95 °C for 0.5 h, then further adding 100 µl H_2O_2 at 95 °C for 1 h, subsequently 75 µl concentrated HCl was added at 95 °C for 0.5 h. The solution was then diluted to a final volume of 1 ml with Milli-Q water. The concentration of ruthenium was determined by Atomic absorption spectrometry (TAS-990, Persee, Beijing, China). The experiment was performed in triplicate, and the average of the data was obtained.

Colocalization assay. A549 cells (5×10^5 /2 ml per well) were seeded in a six-well plate. Cells were preincubated in drug-free media at 310 K for 24 h, after which complexes **Ru1** and **Ru2** was added at concentration $1 \times IC_{50}$ to a six-well plate for different time intervals, and then cells were incubated with MTDR (100 nM) at 310 K for 30 min, 3 h and 12h. Cells were washed three times with ice-cold PBS and visualized by confocal microscopy (LSM 880 NLO, Carl Zeiss, Germany) immediately. Ru complexes were excited at 488 nm and MTDR was excited at 633 nm, respectively. Emission was collected at 520 ± 20 nm (Ru complexes) and 710 ± 20 nm (MTDR), respectively.

Mitochondrial Membrane Assay. Analysis of the changes of mitochondrial potential in cells after exposure to iridium complexes was carried out using the Mitochondrial membrane potential assay kit with JC-1 (Beyotime Institute of Biotechnology, Shanghai, China) according to the manufacturer's instructions. Briefly, 1.0×10^6 A549 cancer cells per well were seeded in six-well plates left to incubate for 24 h in drug-free medium at 310 K in a humidified atmosphere. Drug solutions, at concentrations of $0.5 \times IC_{50}$, $1 \times IC_{50}$ and $2 \times IC_{50}$ of complexes

Ru1 and **Ru2** against A549 cancer cells, were added in triplicate, and the cells were left to incubate for a further 24 h under similar conditions. Supernatants were removed by suction, and each well was washed with PBS before detaching the cells using trypsin-EDTA. Staining of the samples was done in flow cytometry tubes protected from light, incubating for 30 min at ambient temperature. The samples were immediately analyzed by a flow cytometer (ACEA NovoCyte, Hangzhou, China). For positive controls, the cells were exposed to carbonyl cyanide 3-chlorophenylhydrazone, CCCP (5 μM), for 20 min. Data were processed using NovoExpress™ software.

ROS Determination. Flow cytometry analysis of ROS generation in the cells caused by exposure to Ru complexes was carried out using the Reactive Oxygen Species Assay Kit (Beyotime Institute of Biotechnology, Shanghai, China) according to the supplier's instructions. Briefly, 1.0×10^6 A549 cancer cells per well were seeded in a six-well plate. Cells were preincubated in drug-free media at 310 K for 24 h in a 5 % CO_2 humidified atmosphere, for inhibition studies, cells were pre-treated with NAC (10 mM) for 1 h, and then complexes **Ru1** and **Ru2** were added at concentrations of $0.25 \times IC_{50}$ and $0.5 \times IC_{50}$ against A549 cancer cells. After 24 h of drug exposure, cells were washed twice with PBS and then incubated with the DCFH-DA probe (10 μM) at 37 °C for 30 min, and then washed triple immediately with PBS. The fluorescence intensity was analyzed by flow cytometry (ACEA NovoCyte, Hangzhou, China). Data were processed using NovoExpress™ software. At all times, samples were kept under dark conditions to avoid light-induced ROS production.

Caspase 3 and PARP activity assay. Analysis of the activity of Caspase 3 and PARP was measured by flow cytometry. 1.0×10^6 A549 Cells were preincubated in drug-free media at 310 K for 24 h in a 5 % CO_2 humidified atmosphere, for inhibition studies, cells were pre-treated with NAC (10 mM) for 1 h followed by incubation with the tested complexes **Ru1** and **Ru2** at the $1\times IC_{50}$ concentration for 24 h. Then the cells were harvested and stained with specific antibody of cleaved Caspase-3 and PARP according to the manufacturer's instructions. Analysis was performed by NovoExpress™ software.

Wound healing assay. Wound healing assay was performed using A549 cancer cells. Briefly, A549 cells were plated into 6-well plates at a density of 5.0×10^5 cells per well and allowed to grow for 24 h. Then the monolayer cells were wounded by scratching with 20 μl pipette tips and unattached cells washed with PBS. Fresh medium with 1% FBS was used to suppress cell proliferation, then containing complexes **Ru1** and **Ru2** at the $0.5 \times IC_{50}$ concentration in the absence and presence of NAC (10 mM) were added. At specific time intervals (0 h and 24 h), images were taken. The wound width was measured in order to evaluate the wound healing ability of tested cells.

Transwell Migration Assay. Transwell migration assays were performed by using transwell chamber in 24-well cell culture plate with 8 μm pores. Chambers were washed with PBS for three times. Then the 600 μl medium with the tested compounds at concentration of IC_{50} was placed in the lower chamber, and A549 cancer cells (2×10^5/well) in 200 μl serum-free medium were seeded in the top chamber. Cells were treated with complexes **Ru1** and **Ru2** at the $1 \times IC_{50}$ concentration in the absence and presence of NAC (10 mM) at 310 K in a humidified atmosphere of 5% CO_2. After incubation for 24 h, non-migrated cells on the top surface of the membrane were gently scraped away with cotton swab, and migrated cells were fixed with 4% paraformaldehyde for 20 min and stained with 0.1% crystal violet for 30 min. The cells that migrated to the lower side of the membranes were imaged and counted using a microscope.

Binding with BSA. The titration experiments including UV–Vis absorption and fluorescence quenching were performed at constant concentration of BSA. A BSA stock solution was prepared in Tris buffer (5 mM Tris–HCl/10 mM NaCl at pH 7.2) and stored at 4 °C. All spectra were recorded after each successive addition of the compounds and incubation at room temperature for 5 min to complete the interaction. The ruthenium complex was added to both sample cuvette and the reference cuvette in order to offset the self-absorption of iridium complex in the UV region. The fluorescence emission spectra of BSA in the absence and presence of Ru

complex were recorded with excitation at 285 nm. The concentrations of the Ru complex were 0–10 μM, and the concentration of BSA was fixed at 10 μM. Synchronous fluorescence spectra of BSA with various concentrations of complexes (0–10 μM) were obtained from 240 to 500 nm .

In the UV–Vis absorption titration experiment, a BSA solution (2.5 ml, 10 μM) was titrated by successive additions of the stock solutions of Ru complex ($1x10^{-3}$ M) and the changes in the BSA absorption. After 10 min equilibration at room temperature, the absorption spectrum of BSA was recorded for each successive addition of the complex.

The UV-Vis absorption spectra of BSA in the presence of **Ru1** are shown in Fig. **S14**. Complex **Ru1** was added to both the sample cuvette and the reference cuvette in order to offset the self-absorption of **1** in the UV region. After the addition of **Ru1** the absorption peak at 228 nm decreased significantly, which is due to interference to the α-helix of BSA by complex **Ru1**.[1-3] With the addition of **Ru1** to BSA, a progressive decrease without any shift was observed in the absorption peak of BSA at 278 nm, suggesting that the Ru complex interacted with the BSA molecule and the microenvironment of the three aromatic acid residues in BSA (Trp, Tyr and Phe) was altered.[4] Through the study of fluorescence quenching the binding capacity of **Ru1** with BSA was further studied. The fluorescence measured in this work was calibrated to correct the ‘‘inner filter’’ effect.[5] The fluorescence emission spectra of BSA in the presence of complex **Ru1** at various concentrations at 298 K are shown in Fig. **S15**. With an increase in the concentration of complex **Ru1**, the fluorescence intensity of BSA gradually decreased, suggesting that complex **Ru1**can interact with BSA *via* a static quenching mode. The possible quenching mechanism can be interpreted using the Stern–Volmer equation (eqn (1)):[6]

$$F_0/F = 1 + K_{sv}[Q] = 1 + K_q\tau_0[Q] \quad (1)$$

where F_0 and F are the fluorescence intensities in the absence and presence of the quenching agent Q, [Q] represents the concentration of the quenching agent, K_q is the quenching rate constant and τ_0 is the average life expectancy of the fluorescent substance when the quencher does not exist, approximately 10^{-8} s.[7] K_{SV} is the Stern–Volmer constant which can be obtained from the ratio of the slope to the intercept of the plot of F_0/F *versus* the concentration of the tested complex (Fig. **S16**, ESI†). The results are listed in Table **S11**, ESI†. The calculated value of K_q for the complex is 4.2×10^{12} M^{-1} s^{-1}, which is about two orders of magnitude higher than that of the purely dynamic quenching mechanism (2.0×10^{10} M^{-1} s^{-1}).[8] Thus, this value of K_q indicates that a static quenching mechanism dominates in the interaction between the **Ru1** and BSA. The binding constant K_b and the number of complexes bound to BSA (n) are calculated (Fig. **S17,** ESI†) using the following formula (eqn (2)):[9]

$$\log[(F_0-F)/F] = \log K_b + n \log[Q] \quad (2)$$

The magnitudes of K_b and K_q of complex **Ru1** are 10^4 M^{-1} and 10^{12} M^{-1} s^{-1}, respectively, indicating a medium binding ability to BSA.

Notes and References

1. R. Esteghamat-Panah, H. Hadadzadeh, H. Farrokhpour, M. Mortazavi and Z. Amirghofran, *Inorg. Chim. Acta*, 2016, **454**, 184-196.
2. J. Ruiz, C. Vicente, C. D. Haro and D. Bautista, *Inorg. Chem.*, 2013, 52, 974-982.
3. F. Samari, B. Hemmateenejad, M. Shamsipur, M. Rashidi and H. Samouei, *Inorg. Chem.*, 2012, 51, 3454-3464.
4. S. Tabassum, R. Singh, M. Zaki, M. Ahmad and M. Afzal, *Rsc Adv.*, 2015, **5**, 35843-35851.
5. M. E. Pacheco and L. Bruzzone, *J. Lumin.*, 2013, 137, 138-142.
6. A. Castiñeiras, N. Fernández-Hermida, I. García-Santos and L. Gómez-Rodríguez, *Dalton Trans.*, 2012, 41, 13486-13495.
7. R. Pettinari, F. Marchetti, A. Petrini, C. Pettinari, G. Lupidi, B. Fernández, A. R. Diéguez, G. Santoni and M. Nabissi, *Inorg. Chim. Acta*, 2017, 454, 139-148.
8. J. Tang, F. Luan and X. Chen, *Biorg. Med. Chem.*, 2006, 14, 3210-3217.
9. Z. Cheng, *J. Lumin.*, 2012, **132**, 2719-2729.

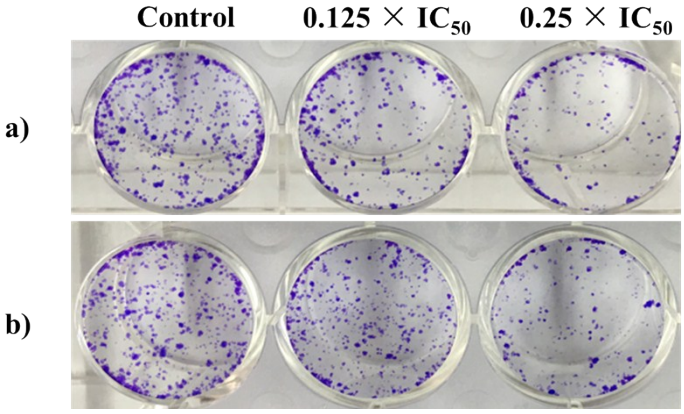

Figure S1. Representative photographs showing colonies of the A549 cells exposed to complexes **Ru1** (a) and **Ru2** (b) for 10 days. Concentrations used were 0.125 and 0.25 equipotent concentrations of IC_{50}.

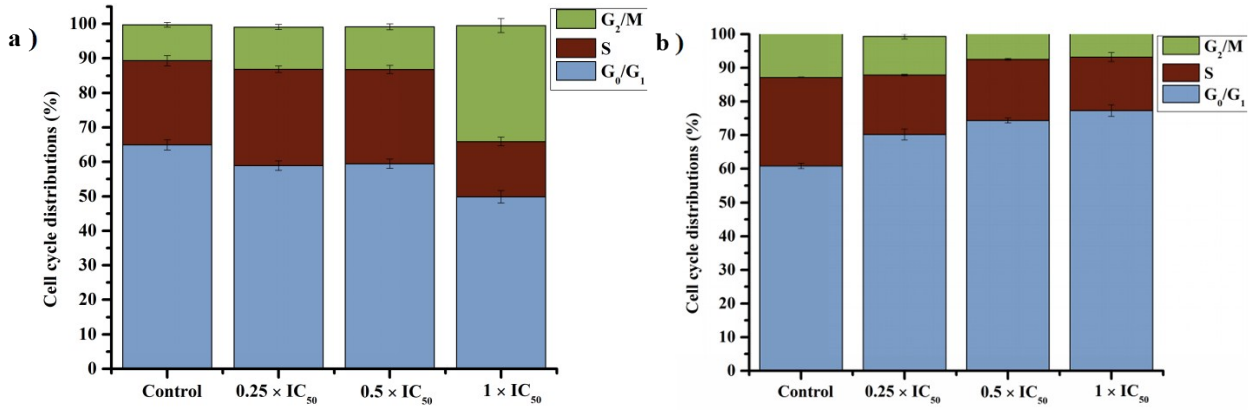

Figure S2. Flow cytometry data for cell cycle distributions of A549 cancer cells exposed to complexes **Ru1** and **Ru2** for 24 h. Concentrations used were 0.25, 0.5, 1 and 2 equipotent concentrations of IC_{50}. Cell staining for flow cytometry was carried out using PI/RNase. Data are quoted as mean ± SD of three replicates.

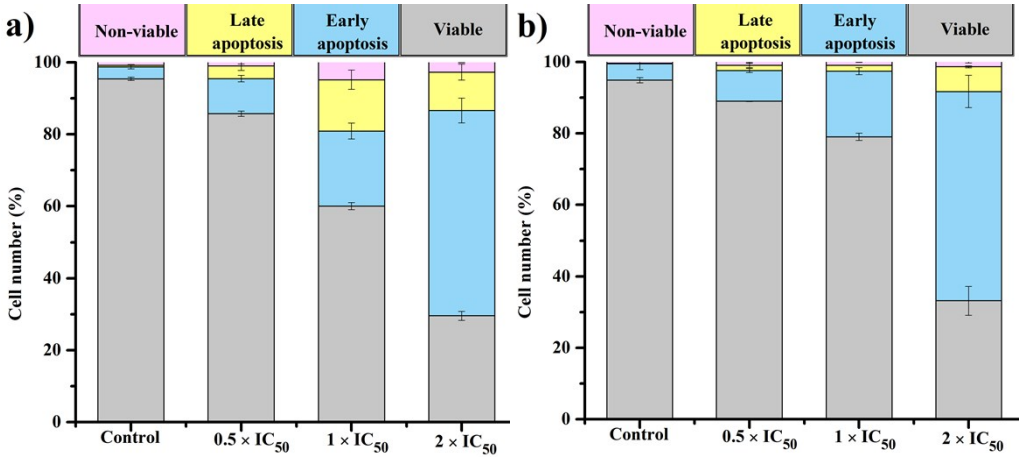

Figure S3. Apoptosis analysis of A549 cells after 24 h of exposure to complexes **Ru1** (a) and **Ru2** (b) at 310 K determined by flow cytometry using annexin V-PE/7-AAD staining. Data are quoted as mean ± SD of three replicates.

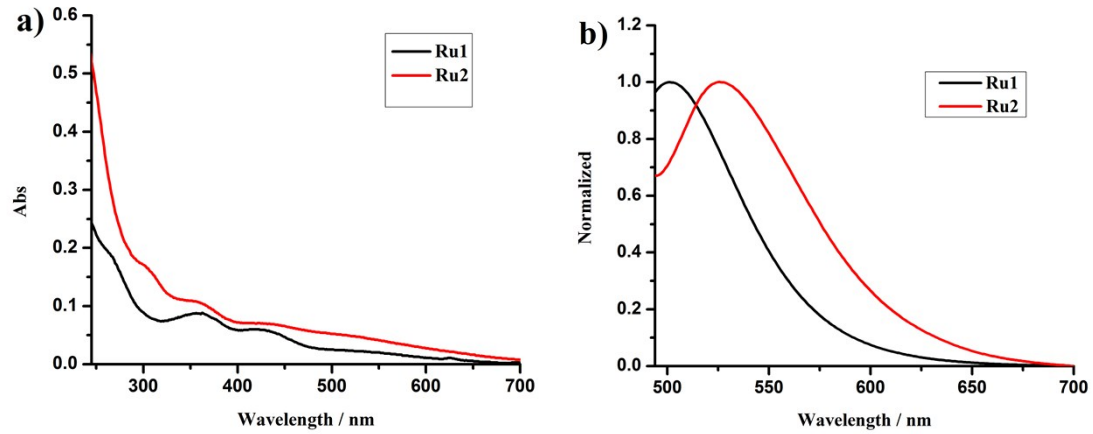

Figure S4. UV/Vis spectra of **Ru1** and **Ru2** (10 μM) measured in CH_2Cl_2 at 298 K (a). Emission spectra of **Ru1** and **Ru2** (10 μM) measured in CH_2Cl_2 at 298 K upon excitation at 420 nm (b).

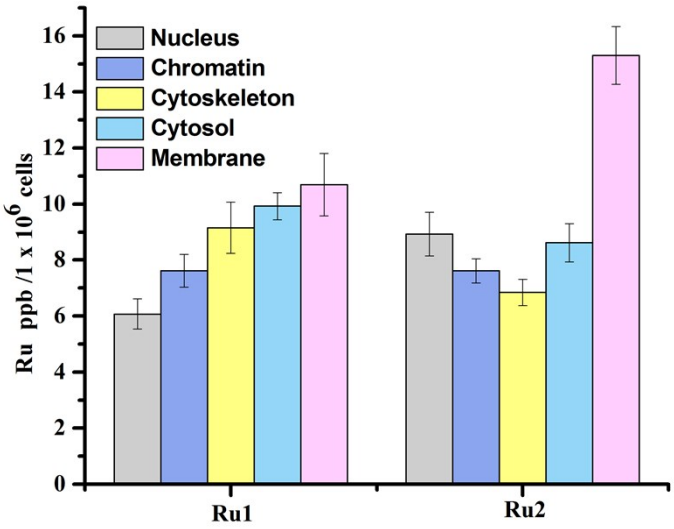

Figure S5. Ru content of the nucleus, chromatin, cytosol, membrane, and cytoskeleton fractions (ppb Ru / 1 × 10^6 cells) of A549 cells after 24 h of exposure to complexes **Ru1** and **Ru2** (10μM). Results are the means of two independent experiments in triplicate and are expressed as means mean ± SD.

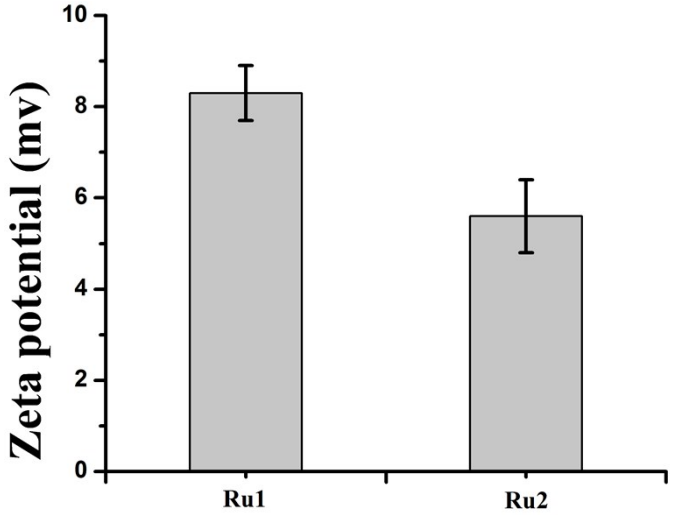

Figure S6. The Zeta potentials of **Ru1** (0.1mg/ml) and **Ru2** (0.1mg/ml) in EtOH at 298k.

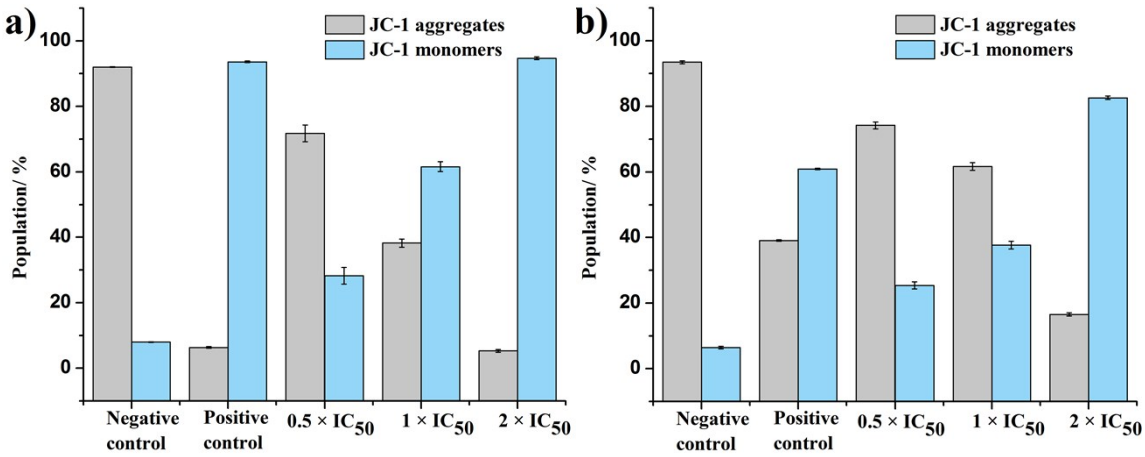

Figure S7. Changes in mitochondrial membrane potential of A549 cancer cells induced by complexes **Ru1** (a) and **Ru2** (b) at concentrations of 0.5 × IC_{50}, 1 × IC_{50} and 2 × IC_{50}. Populations of cells that exhibit a reduction in the mitochondrial membrane potential. Data are quoted as mean ± SD of three replicates.

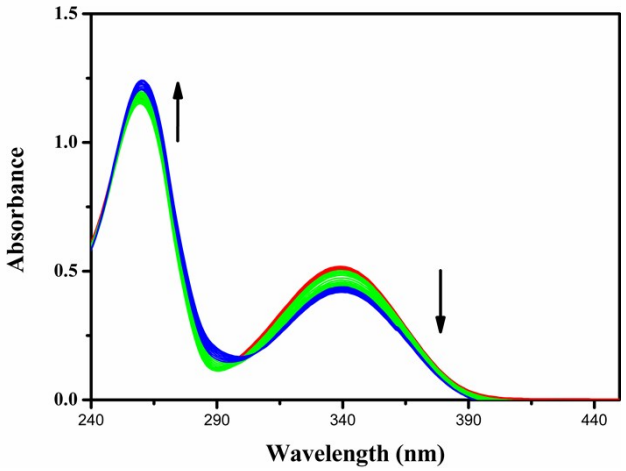

Figure S8. UV-Vis spectra of the reaction of NADH (83 μM) with complex **Ru1** (1 μM) in 10% MeOH/90% H_2O (v/v) at 298 K for 8 h.

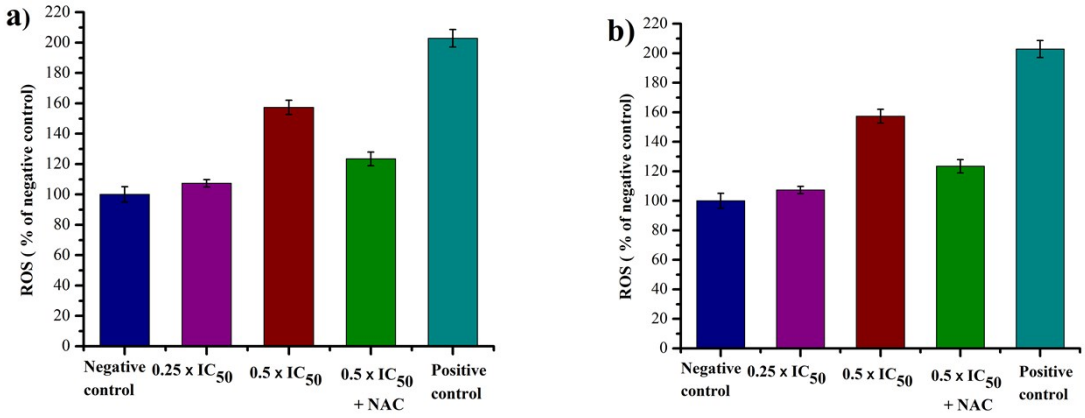

Figure S9. Flow cytometric analysis of Ru complexes induced ROS generation. A549 cells stained with DCFH-DA after treatment by various concentrations of complexes **Ru1** (a) and **Ru2** (b) for 24 h. For inhibition studies, cells were pre-treated with NAC (10 mM) for 1 h.

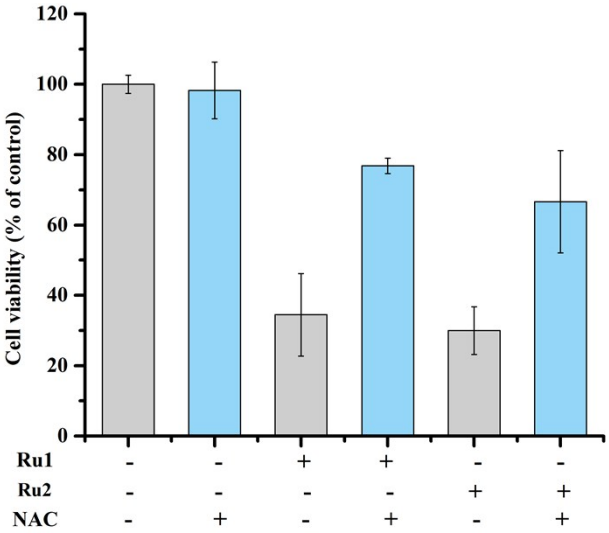

Figure S10. NAC (10 mM) reduced the antiproliferative activity of complexes **Ru1** and **Ru2** at the concentration of 2 × IC_{50} in A549 cells treated for 24 h. Data are quoted as mean ± SD of three replicates.

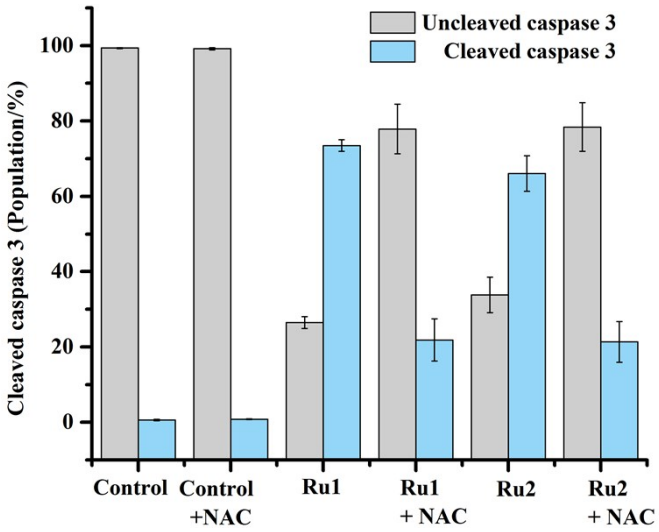

Figure S11. NAC (10 mM) reduced the activation of caspase 3 which was caused by complexes **Ru1** and **Ru2** at concentration of 1 × IC_{50} in A549 cells. Data are quoted as mean ± SD of three replicates.

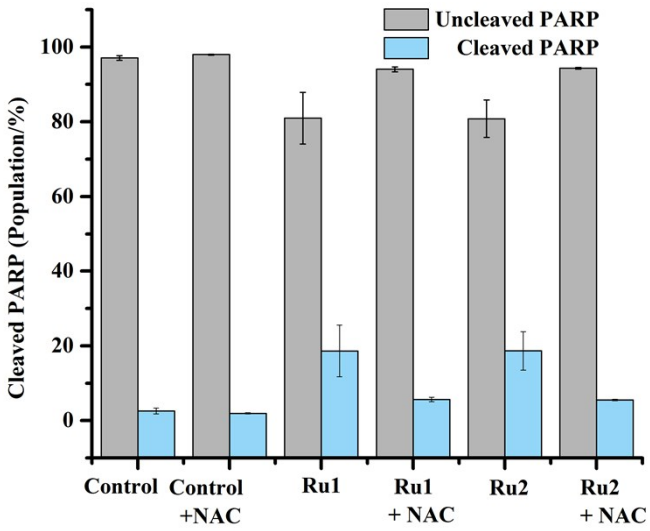

Figure S12. NAC (10 mM) reduced the activation of PARP which was caused by complexes **Ru1** and **Ru2** at concentration of 1 × IC_{50} in A549 cells. Data are quoted as mean ± SD of three replicates.

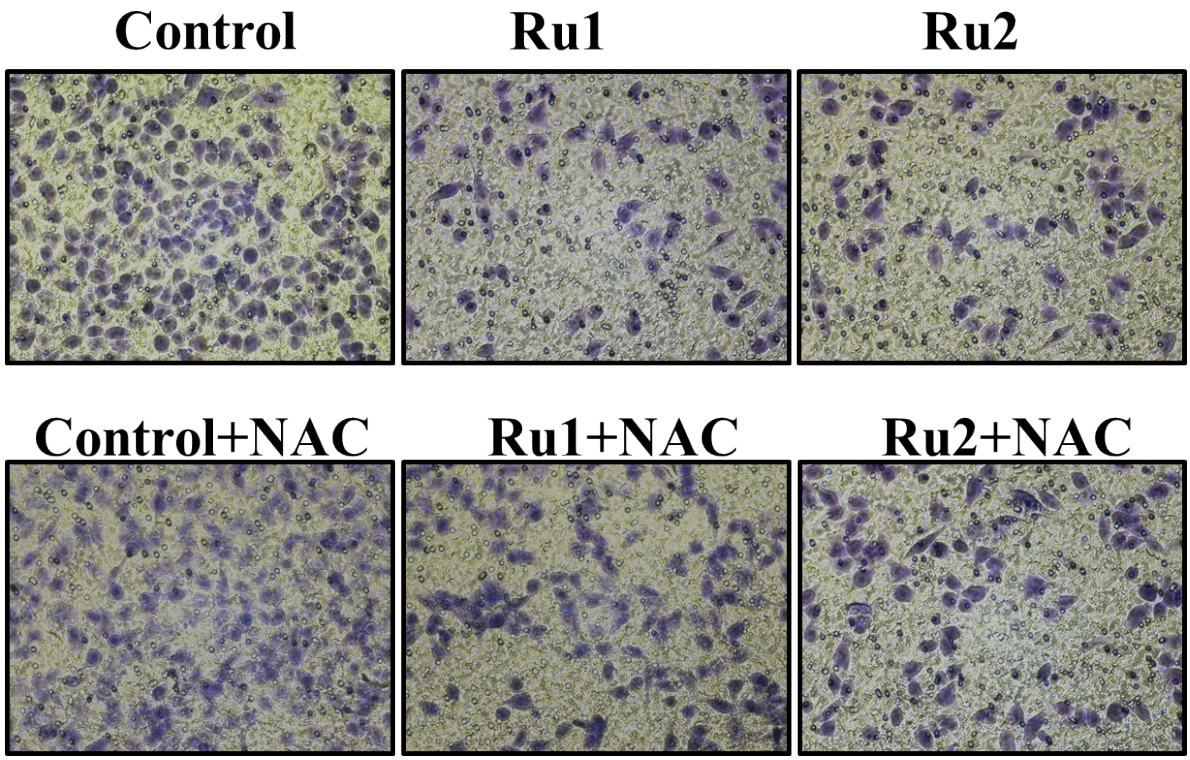

Figure S13. NAC (10 mM) pretreatment weakened the inhibitory effect of complexes **Ru1** and **Ru2** on the migration of A549 cells.

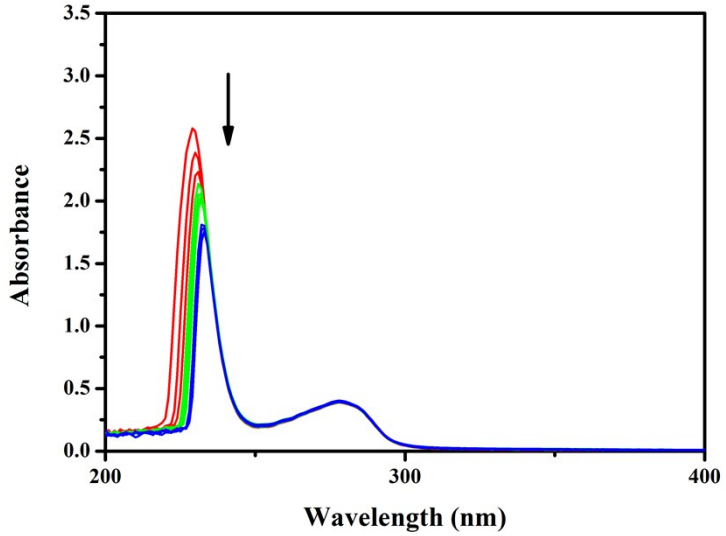

Figure S14. UV-Vis spectra of the reaction of BSA (5 mM) with different concentrations of complex **Ru1**. The arrow shows the absorbance changes upon increasing the concentration of complex **Ru1**.

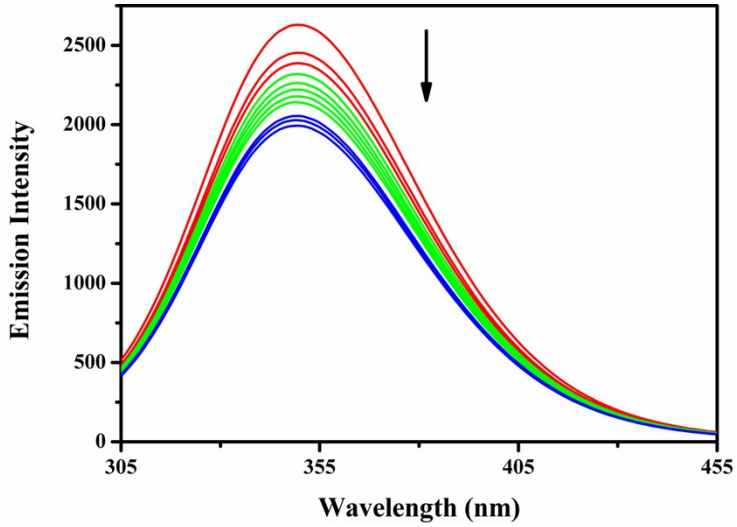

Figure S15. Emission spectra of BSA (10 mM; lex =280nm; lem =343nm) in the presence of increasing amounts of **Ru1**. The arrow shows that the emission intensity changes when the concentration of the complex **Ru1** is increased.

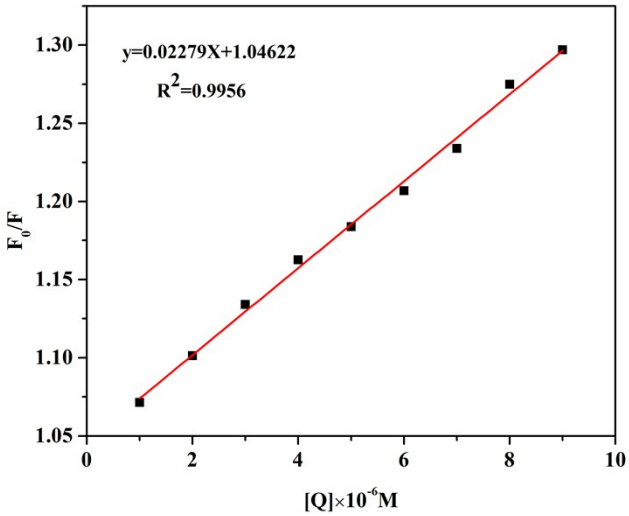

Figure S16. Stern-Volmer plots of F_0/F against the concentration of **[(η⁶-p-cymene)Ru(L₁)Cl]PF₆** (**Ru1**).

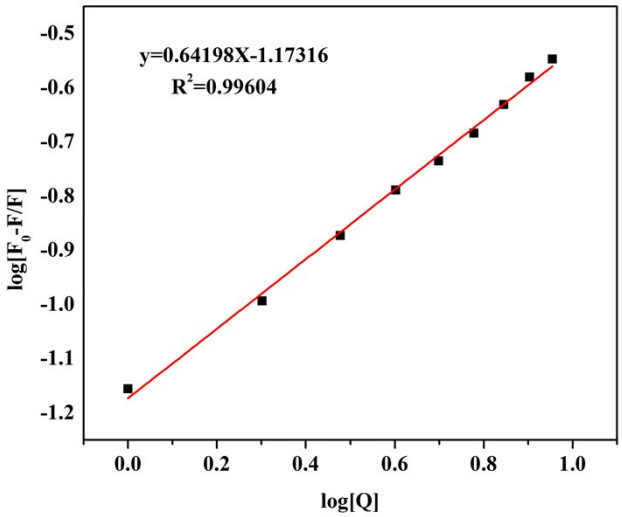

Figure S17. Plots of log [(F_0-F)/F] vs. log [Q] for the interaction of BSA with **[(η⁶-p-cymene)Ru(L₁)Cl]PF₆** (**Ru1**).

Table S1. Cell cycle analysis carried out by flow cytometry using PI staining after exposing A549 cells to complex **Ru1**.

		Population (%)		
Complex	**Ru concentration**	**G_0/G_1 phase**	**S phase**	**G_2/M phase**
Ru1	0.25 × IC_{50}	58.9±1.4	27.9±0.9	12.2±0.7
	0.5 × IC_{50}	59.4±1.3	27.4±1.1	12.3±0.8
	1 × IC_{50}	49.8±1.8	16.0±1.3	33.6±2.0
control		64.9±1.5	24.4±1.5	10.4±0.7

Table S2. Cell cycle analysis carried out by flow cytometry using PI staining after exposing A549 cells to complex **Ru2**.

		Population (%)		
Complex	**Ru concentration**	**G_0/G_1 phase**	**S phase**	**G_2/M phase**
Ru2	0.25 × IC_{50}	70.2±1.6	17.7±0.3	11.5±0.7
	0.5 × IC_{50}	74.3±0.7	18.2±0.3	7.5±0.6
	1 × IC_{50}	77.3±1.7	15.9±1.4	7.0±0.5
control		60.8±0.8	26.3±0.1	12.8±0.6

Table S3. Flow cytometry analysis to determine the percentages of apoptotic cells, using Annexin V-PE and 7-AAD staining, after exposing A549 cells to complex **Ru1**.

		Population (%)			
Complex	**Ru concentration**	**Viable**	**Early apoptosis**	**Late apoptosis**	**Non-viable**
Ru1	0.5 × IC_{50}	85.7±0.7	9.8±0.9	3.5±1.2	1.0±0.4
	1 × IC_{50}	60.0±0.9	20.9±2.2	14.3±2.6	4.8±0.5
	2 × IC_{50}	29.5±1.2	57.1±3.4	10.7±2.2	2.7±0.1
control		93.4±0.4	1.1±0.9	3.7±0.9	1.8±0.4

Table S4. Flow cytometry analysis to determine the percentages of apoptotic cells, using Annexin V-PE and 7-AAD staining, after exposing A549 cells to complex **Ru2**.

		Population (%)			
Complex	**Ru concentration**	**Viable**	**Early apoptosis**	**Late apoptosis**	**Non-viable**
Ru2	$0.5 \times IC_{50}$	89.0±0.1	8.6±0.6	1.5±0.6	0.9±0.1
	$1 \times IC_{50}$	79.1±1.0	18.4±0.9	1.6±0.1	0.9±0.1
	$2 \times IC_{50}$	33.1±4.0	58.6±4.5	6.9±0.3	1.3±0.2
control		94.9±1.5	4.6±1.6	0.2±0.1	0.3±0.1

Table S5. The mitochondrial membrane polarization of A549 cells induced by complex **Ru1**.

		Population (%)	
Complex	**Ru concentration**	**JC-1 Aggregates**	**JC-1 Monomers**
Ru1	$0.5 \times IC_{50}$	71.8±2.5	28.2±2.4
	$1 \times IC_{50}$	38.2±1.3	61.6±1.5
	$2 \times IC_{50}$	5.3±0.4	94.7±0.3
Negative control		91.9±0.1	7.9±0.1
Positive control		6.3±0.3	93.6±0.2

Table S6. The mitochondrial membrane polarization of A549 cells induced by complex **Ru2.**

		Population (%)	
Complex	**Ru concentration**	**JC-1 Aggregates**	**JC-1 Monomers**
Ru2	$0.5 \times IC_{50}$	74.1±1.0	25.3±1.1
	$1 \times IC_{50}$	61.6±1.2	37.6±1.2
	$2 \times IC_{50}$	16.5±0.5	82.6±0.6
Negative control		93.4±0.4	6.4±0.3
Positive control		39.0±0.3	60. 9±0.2

Table S7. NAC (10 mM) reversed complex **Ru1** - elevated ROS level in A549 cells.

Complex	Ru concentration	ROS (% negative control)
Ru1	0.25 × IC_{50}	128.7±7.9
	0.5 × IC_{50}	160.8±0.3
	0.5 × IC_{50} + NAC	131.4±1.2
Untreated cells (Negative control)		100.0±8.8
CCCP treated cells (Positive control)		157.3±2.9

Table S8. NAC (10 mM) reversed complex **Ru2** - elevated ROS level in A549 cells.

Complex	Ru concentration	ROS (% negative control)
Ru2	0.25 × IC_{50}	107.3±2.4
	0.5 × IC_{50}	157.3±4.7
	0.5 × IC_{50} + NAC	123.4±4.5
Untreated cells (Negative control)		100.0±5.1
CCCP treated cells (Positive control)		202.8±5.7

Table S9. NAC (10 mM) reduced the caspase 3 activation in A549 cells caused by 24 h exposure to complexes **Ru1** and **Ru2** at concentration of 1 × IC_{50}.

	Population (%)	
Complex	**Uncleaved caspase 3**	**Cleaved caspase 3**
Control	99.3±0.1	0.7±0.1
Control + NAC	99.2±0.2	0.8±0.1
Ru1	26.4±1.6	73.5±1.5
Ru1 + NAC	77.8±6.0	21.9±5.6
Ru2	33.8±4.5	66.1±4.3
Ru2 + NAC	78.3±6.5	21.3±5.4

Table S10. NAC (10 mM) reduced the PARP activation in A549 cells caused by 24 h exposure to complexes **Ru1** and **Ru2** at concentration of 1 × IC_{50}.

	Population (%)	
Complex	**Uncleaved PARP**	**Cleaved PARP**
Control	97.1±0.6	2.5±0.8
Control + NAC	97.9±0.1	1.9±0.1
Ru1	80.9±6.9	18.6±6.8
Ru1 + NAC	94.1±0.6	5.6±0.5
Ru2	80.7±5.1	18.7±5.2
Ru2+ NAC	94.3±0.3	5.5±0.2

Table S11. Quenching parameters and binding parameters for the interaction of the complex **Ru1** with BSA.

Complex	**T (K)**	**K_{sv} (10^4 M^{-1})**	**K_q (10^{12} $M^{-1}s^{-1}$)**	**K_b (M^{-1})**	**n**
Ru1	298	4.2±0.6	4.2	6.7×10^4	0.6